Journal of Thermal Analysis, Vol. 49 (1997) 499-511

SEPARATION OF COMPONENTS OF DIFFERENT MOLECULAR MOBILITY BY CALORIMETRY, DYNAMIC MECHANICAL AND DIELECTRIC SPECTROSCOPY

C. Schick[a], *J. Dobbertin*[a], *M. Pötter*[b], *H. Dehne*[b], *A. Hensel*[a], *A. Wurm*[a], *A. M. Ghoneim*[c] *and S. Weyer*[a]

[a]University of Rostock, Department of Physics, Universitätsplatz 3, 18051 Rostock
[b]University of Rostock, Department of Chemistry, Buchbinderstr. 9, 18051 Rostock, Germany
[c]National Research Center, Physics Department, Dokki, Cairo, Egypt

Abstract

The relaxation strength at the glass transition for semi-crystalline polymers observed by different experimental methods shows significant deviations from a simple two-phase model. Introduction of a rigid amorphous fraction, which is non-crystalline but does not participate in the glass transition, allows a description of the relaxation behavior of such systems. The question arises when does this amorphous material vitrify. Our measurements on PET identify no separate glass transition and no devitrification over a broad temperature range. Measurements on a low molecular weight compound which partly crystallizes supports the idea that vitrification of the rigid amorphous material occurs during formation of crystallites. The reason for vitrification is the immobilization of co-operative motions due to the fixation of parts of the molecules in the crystallites. Local movements (β-relaxation) are only slightly influenced by the crystallites and occur in the whole non-crystalline fraction.

Keywords: dielectric spectroscopy (DETA), DSC, dynamic mechanical (DMA) spectroscopy, glass transition, PET, polymers, relaxation, rigid amorphous, temperature modulated DSC

Introduction

By varying the morphology of a semi-crystalline polymer one can investigate whether and how both the thermal (vitrification) and the dynamic (relaxation) glass transition are influenced. As given by Ishida [1] for dielectric and Wunderlich [2] for calorimetric investigations, the fraction (χ_{am}) participating in the glass transition can be determined by the strength of the relaxation process under investigation ($\Delta\varepsilon$; Δc_p; ΔJ_a;...) as

$$\chi_{am\varepsilon} = \frac{\Delta\varepsilon}{\Delta\varepsilon_a}; \quad \chi_{amc_p} = \frac{\Delta c_p}{\Delta c_{pa}}; \quad \chi_{amJ} = \frac{\Delta J}{\Delta J_a} \tag{1}$$

where $\Delta\varepsilon$, Δc_p, ΔJ are relaxation strength for permittivity, heat capacity and mechanical compliance, respectively of the investigated sample. The subscript "*a*" in

0368–4466/97/ $ 5.00

John Wiley & Sons Limited
Chichester

the denominator means the corresponding value of the fully amorphous sample. From independent measurements like wide-angle X-ray scattering (WAXS), density, melting enthalpy,...etc. the crystalline fraction χ_c can be determined. For polymers, the mobile amorphous fraction (χ_{am}) is less than the non-crystalline fraction ($1-\chi_c$), so Wunderlich [2] introduced a third fraction which is non-crystalline but does not participate in the common glass transition. It is called rigid amorphous (χ_{ar}).

$$\chi_{ar} = 1 - \chi_c - \chi_{am} \tag{2}$$

The questions arise: Does this fraction exhibit a separate glass transition at higher temperatures? Is it smeared over a broad temperature range? Is the devitrification a part of the melting of crystals [3]? Another interesting question is that of possible differences between the values determined via Eqs (1) and (2) by different methods.

We will thus compare the results from calorimetric investigations of the vitrification process with those of dynamic experiments performed on the metastable, super-cooled state of semi-crystalline poly(ethylene-terephthalate) (PET). Since vitrification temperature (T_g) depends on cooling rate while dynamic glass transition temperature (T_{gHz}) depends on frequency, it is possible to investigate the relaxation strength at different temperatures. From such investigations we will try to obtain information about the temperature dependence of the different fractions resulting from (1) and (2). In our laboratory we cover a frequency range from 10^{-5} to 10^9 Hz for dielectric spectroscopy and from 10^{-4} to 100 Hz for mechanical spectroscopy. In the case of PET we are able to shift the dynamic glass transition temperature about 40 K by varying the frequency over 8 decades.

Using dielectric and mechanical spectroscopy we can additionally observe the low temperature (local, secondary, β-) relaxation. The low temperature relaxation is connected with local movements, whereas the glass transition should be connected with co-operative movements [4, 5]. According to Eq. (1) we can calculate the mobile amorphous fraction related to the local movements from the relaxation strength of the β-relaxation. We compare the results with that of the dynamic glass transition (main-, α-relaxation) [6].

The common picture is that the rigid amorphous fraction, observed in semi-crystalline polymers, is the result of restrictions of molecular mobility due to the fixation of the polymer chain at the surface of the crystalline lamellae. This paper presents an example for a rigid amorphous fraction in a low molecular weight compound directly related to the formation of a small amount of crystallites.

Experimental

Poly(ethylene-terephthalate) PET allows variation of morphology over a wide range and study of its influence on the relaxation behavior. Using different temperature-time programs, one can generate semi-crystalline structures with different morphologies [7–10].

Sample preparation

From one PET batch (ORWO K 36, $\overline{M_w} \approx 23000$) we prepared two series of samples with a variation of crystalline, rigid amorphous and mobile amorphous fraction between 0.25–0.35, 0.32–0.43 and 0.2–0.35, respectively.

The first sample series was prepared by isothermal crystallization in the temperature range T_c=393 K to T_c=493 K (3...18 h dependent on the growth rate). The samples were crystallized to the end of primary crystallization to get samples totally filled with lamellae stack structures (as totally as possible for a given T_c). The crystallization was stopped when the sample was totally filled with such lamellae stack structures to avoid secondary crystallization. This allows us to take into account only intra-spherulitic amorphous regions and to neglect inter-spherulitic amorphous regions [11, 12]. Both long period L and crystallinity χ_c increase with increasing T_c [9].

The second series was prepared by gradual crystallization according to Groeninckx [10]. First, the sample was completely crystallized (18 h) at T_c=393 K. Then, the sample was heated at the rate of q=0.1 K min^{-1} up to the next annealing temperature, e.g. T_a=413 K, at which the sample was additionally annealed for a period of 18 h. After that, the sample was heated again at the same rate q up to the next annealing temperature T_a and again annealed for 18 h. This procedure was repeated until the final annealing temperature T_a was reached. As shown in [7] and [10] in the gradual crystallized series no variation of the long period, fixed by the first annealing at 393 K, can be observed for T_a less than 493 K. The crystallinity χ_c increases with increasing annealing temperature similar to the first series.

The low molecular weight compound investigated is 2,5-bis(2-dodecyloxycarbonyl-phenylthio)terephthalic dodecyl diester. Synthesis of this and homologues are described elsewhere [13]. The chemical structure is shown in Fig. 1.

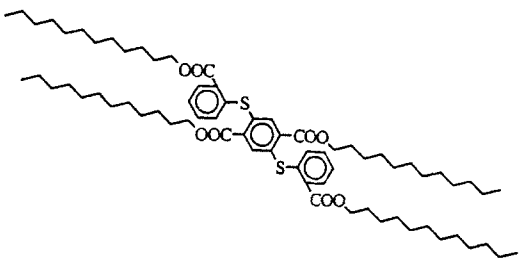

Fig. 1 2,5-bis(2-dodecyloxycarbonyl-phenylthio)terephthalic dodecyl diester

Differential scanning calorimetry (DSC)

Vitrification, that means the change from a meta-stable equilibrium of a supercooled liquid to a non-equilibrium state of a glass, was investigated by DSC measurements on cooling using either a Perkin-Elmer DSC-2 or a DSC-7. Figure 2 shows typical DSC traces in the glass transition region of different crystallized PET samples.

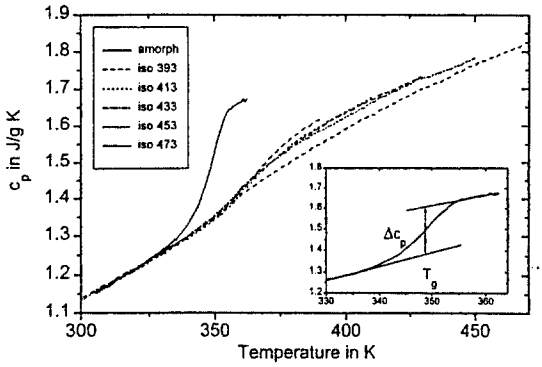

Fig. 2 Standard DSC measurements of different isothermal crystallized PET samples. iso 393 ... iso 473 – crystallizaton temperature 393 K ... 473 K, respectively. Measuring conditions see text

The temperature scale of the calorimeter was calibrated with indium and lead for the scanning rate used and for the heat flow by sapphire. The purge gas was nitrogen. The temperature of the calorimeter block as well as the room temperature were kept well stabilized at temperatures of (198±0.1) K and (300±0.5) K respectively, in order to realize reproducible scans. Sample mass was about 12 mg and the scanning rate was 10 K min^{-1} for both heating and cooling. The glass transition temperature T_g of the compounds was taken as the midpoint temperature. The midpoint temperature is usually defined as the temperature of the half step-height Δc_p at the glass transition, see inset in Fig. 2.

With temperature modulated calorimetry (TMC) like third harmonic detection [14, 15], photoacoustic methods (PA) [16], light heating DSC [17] or temperature modulated DSC (TMDSC) [18, 19] frequency dependent heat capacity can be determined in the temperature range of the meta-stable equilibrium in the supercooled state. With these methods it is possible to perform heat capacity spectroscopy. We used a Perkin-Elmer DDSC-7 and a Setaram DSC 121 to determine the complex heat capacity in the glass transition range (Fig. 3).

The following measurement conditions were chosen unless otherwise stated: saw tooth modulation with modulation frequency 0.017 Hz (modulation period 1 min); temperature amplitude 0.2 K; underlying cooling rate 0.8 K min^{-1}; sample mass ca. 12 mg; temperature calibration for temperature modulated mode by liquid crystal phase transition [20]; heat flow calibration by poly(ethylene-terephthalate) at 300 K according to the ATHAS data bank [21].

Because the modulation frequency available with TMDSC is low (10^{-1} to 10^{-4} Hz) [22], some overlapping of vitrification and the dynamic glass transition occurs which slightly influences the dynamic glass transition [23]. To reduce the influence of vitrification on the dynamic glass transition, additional quasi-isothermal measurements [24] were performed using the Setaram DSC 121. Also, comparison of the results from quasi-isothermal and scanning measurements allows observation of the possible influence of melting or crystallization on the determined heat capacity values.

As seen from Fig. 3, there are no differences between the values above the glass transition. That means, no melting below the crystallization temperature occurs.

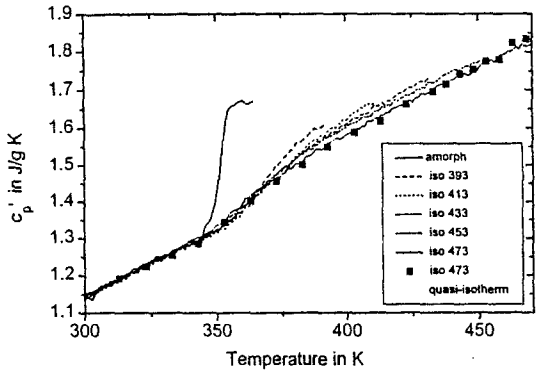

Fig. 3 Temperature Modulated DSC measurements. Samples as in Fig. 2. Measuring conditions see text. The quasi-isothermal measurements (■) has been performed with a Setaram DSC 121. Modulation period 600 seconds; modulation amplitude 0.1 K; sample mass 273 mg

Due to the very broad glass transition region in semi-crystalline PET the precision of the common TMDSC apparatus is not high enough to obtain reliable values of phase shift δ due to the glass transition and consequently the tan(δ) or the imaginary part of the heat capacity. For detailed information on complex heat capacity and its determination see e.g. [14, 15, 19, 22] and references therein. To obtain information on the relaxation strength of heat capacity, we used the real part of the complex heat capacity. Figure 3 shows typical curves for different crystallized PET samples.

Dielectric measurements (DETA)

The dielectric measurements were carried out in the frequency range 0.01 Hz to 1 MHz with a BDS 4000 Broadband Dielectric Spectrometer (Novocontrol GmbH). A frequency response analyzer SI 1260 (Solatron-Schlumberger), which was supplemented by a high-impedance preamplifier of variable gain, was used to extract the complex dielectric function

$$\varepsilon^*(f) = \varepsilon'(f) - i\varepsilon''(f) \tag{3}$$

with f – frequency, ε' – real part, ε'' – imaginary part. The samples with a thickness of approximately 100 μm were kept in a cryostat where the sample temperature was controlled using a nitrogen gas stream of controlled temperature. Frequency scans were performed at constant temperature, with a temperature stability better than 0.1 K [25].

Figure 4 shows typical frequency scans for PET isothermally crystallized at 433 K. The measured dielectric function for a relaxation process can be described quantitatively by generalized relaxation functions. A general one is the Havriliak-Negami (HN) equation [26]:

$$\varepsilon^*(f) = \varepsilon_\infty + \Delta\varepsilon\left[1 + (if/f_c)^\beta\right]^{-\gamma} \quad (0<\beta,\ \beta\gamma \leq 1) \tag{4}$$

β and γ are shape parameters; f is the frequency of applied field; f_c the characteristic relaxation frequency; and, $\Delta\varepsilon = \varepsilon_{st} - \varepsilon_\infty$ the relaxation strength ($\varepsilon_{st} = \varepsilon'(f)$ for $f \ll f_c$; $\varepsilon_\infty = \varepsilon'(f)$ for $f \gg f_c$).

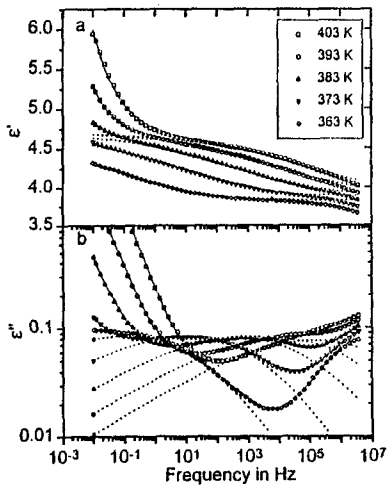

Fig. 4 Real (a) and imaginary (b) part of the complex dielectric function in the glass transition region of PET for the sample isothermally crystallized for 3 h at 433 K. Measuring temperature as parameter. The solid lines through the data represent the fit using two superimposed HN-functions (Eq.(4)) (α- and β-relaxation) and $A_1 f^{-n_1}$ for the Maxwell-Wagner-Sillars-polarization or $A_2 f^{-n_2}$ for conductivity for the real (a) and the imaginary (b) part, respectively. The parameters for α–and β–relaxation used in Figs 4a and 4b are the same. The dashed lines show the HN-fit for the α-relaxation

The α-relaxation is influenced by neighboring processes, conductivity on the low frequency tail and secondary relaxation on the high frequency tail. These processes must be included in the fitting procedure [27] to obtain correct values for the relaxation strength. The curves in Fig. 4 are fitted with a superposition of two HN-functions (for α- and β-relaxation, respectively) and a term describing the conductivity or the surface polarization. The dotted line in Fig. 4 represents the HN-function for the α-relaxation. Both, the imaginary and the real part of the dielectric function are used for fitting.

Dynamic mechanical spectroscopy (DMA)

For the dynamic mechanical spectroscopy we used an ARES spectrometer from Rheometric Scientific. We measured the resultant torque expended by the sample in response to the shear strain. The rectangular samples (35 mm×10 mm×1 mm) were temperature controlled in an oven by using pressured air, an air chiller for mechanical

refrigeration and two heaters. The temperature was calibrated using water, indium and tin by adding a small solid sample in between two half polymer samples and measuring the change in sample length during melting due to a small compression.

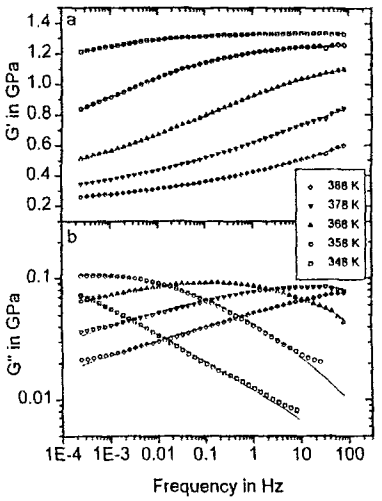

Fig. 5 Real (a) and imaginary (b) part of the complex mechanical modulus in the glass transition region of PET for the sample isothermally crystallized for 3 h at 433 K. Measuring temperature as parameter. The solid lines through the data represent the fit using a modified HN-function (Eq. (5)). The parameters used in Figs 5a and 5b are the same

At different constant temperatures between 198 K and the crystallization temperature of the sample under investigation we performed frequency sweeps in the range of $1.6 \cdot 10^{-4}$ to 80 Hz. Figure 5 shows the real and imaginary parts of the mechanical modulus for the same sample as in Fig. 4. Since it is difficult to compare relaxation strength from DMA with that of DSC and DETA, one must be sensitive to choose the comparable values. Because c_p and ε are compliances we have to determine relaxation strength from mechanical compliance (J) too. From our measurements at first, we plotted modulus G as a function of frequency and determined relaxation strength ΔG from a fit of a modified HN-function [28] (Fig. 5).

$$G^*(f) = G_\infty + \Delta G \left[1 + (-if_c/f)^\beta\right]^{-\gamma} \qquad (0<\beta,\ \beta\gamma\leq 1) \tag{5}$$

where β and γ are shape parameters; G^* is complex mechanical modulus; f is frequency of applied strain and f_c is the characteristic relaxation frequency; and, $\Delta G = G_\infty - G_0$ the relaxation strength ($G_\infty = G'(f)$ for $f \gg f_c$; $G_0 = G'(f)$ for $f \ll f_c$).

Because $J^*G^* = 1$ we can derive relaxation strength ΔJ from ΔG according to

$$\Delta J = \frac{\Delta G}{G_0 G_\infty} \tag{6}$$

Results and discussion

The comparison of vitrification and dynamic glass transition for PET from the different measurements shows a similar behavior. In all experiments we found that the relaxation strength (Δc_p, $\Delta\varepsilon$, ΔJ) of the non-crystalline fraction ($1-\chi_c$) of the samples are smaller than those expected from the two phase model. In Fig. 6 the normalized relaxation strength (mobile amorphous fraction according to Eq. (1)) from the different methods is plotted against crystallinity. Line A represents a two-phase model including crystalline and non-crystalline amorphous fractions only. The points from the low temperature relaxation follow this model whereas the points from the glass transition deviate significantly. The difference between line A and the points at a given crystallinity indicate a non-crystalline fraction, which does not contribute to the relaxation intensity (rigid amorphous, Eq. (2)). Comparing the results from dielectric, calorimetric and mechanical measurements we observe a decreasing mobile amorphous fraction (normalized relaxation strength). This may be related to the different co-operativity of the corresponding movements.

Taking into account that we have investigated only samples crystallized at least until the end of primary crystallization, no bigger (100 nm and larger) melt like amorphous regions in between spherulites must be taken into account [12]. Therefore the different values for the rigid amorphous fraction between 0.32 and 0.43 are due to variations inside the lamellar structure (spherulites).

There are other results which suppose that the found differences from the two-phase model are due to wrong determination of crystallinity [29]. To test this, we have determined the dielectric strength of the low temperature relaxation process (β-relaxation) by dielectric and dynamic mechanical measurements. As generally accepted, the β-relaxation is related to local movements of the main chain or of lateral groups. Such local movements could be expected to occur in the whole non-crystalline part because these movements are only slightly influenced by the confining crystalline lamellae. That's why the secondary relaxation should follow a two-

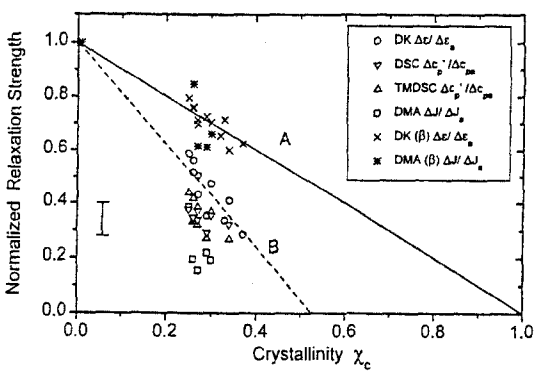

Fig. 6 Normalized relaxation strength for all samples and different measurements as a function of crystallinity. Line A corresponds to a two-phase model and the dashed line B is a guide for the eyes for the results from dielectric measurements

phase model ($\Delta\varepsilon_\beta$; $\Delta J_\beta \propto 1-\chi_c$). Line A in Fig. 6 represents the normalized relaxation strength for a two-phase model. The points for the β-relaxation lie on this line. For the β-relaxation a two-phase model seems to be correct and the measured points fit the model, so the determination of crystallinity can not be totally wrong. Consequently, the deviations from the two-phase model for the α-relaxation must be the result of a rigid amorphous fraction. In the rigid amorphous fraction a local movement is possible but not a co-operative segmental motion (α-relaxation, glass transition).

To test whether there is a separate glass transition of the rigid amorphous fraction at higher temperatures, we performed DETA, DMA, DSC, TMDSC and quasi-isothermal TMDSC measurements over a wide frequency or temperature range. As shown in Figs 4 and 5 the relaxation spectra is very broad (half width more than 6 decades in frequency). Additionally problems especially for DETA result from the superposition of the α-relaxation by neighboring processes. So, for the DETA this must be taken into account (Fig. 4). Uncertainties in the shape parameters and also the relaxation strength remain. Over the entire frequency range only one broad peak was observed for the α-relaxation without large changes in the shape parameters [30]. If there are separate processes in the rigid amorphous fraction a small separation of the second process or at least a change in the curve shape should occur at different frequency positions of the loss peak. Our measurements yield a shift of 8 decades with increasing temperature but we do not observe any indication of a second process. This finding is somewhat different from that found by Kremer and coworkers [31, 32] for low molecular weight glass forming liquids confined in porous glasses. They found two superimposed relaxation processes in the dynamic glass transition region which are well separated in frequency. One related to the α-relaxation and the other to a "interfacial" relaxation due to the inner surface.

In Fig. 7 the relaxation strengths from DETA and DMA are plotted as a function of temperature. Normally for the amorphous sample, a decrease of relaxation strength with increasing temperature can be observed. Our measurements from the semi-crystalline PET yield a nearly constant value for the relaxation strength. This is contrary to some other investigations [33, 34]. As shown in [30] the separation of

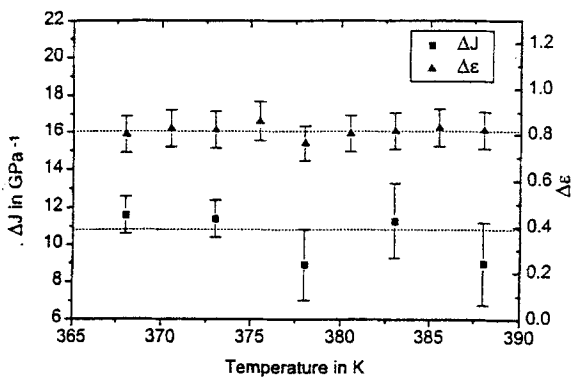

Fig. 7 Relaxation strength from isothermal DETA (10^{-2} Hz$<f<10^6$ Hz) and DMA (10^{-4} Hz$<f<10^2$ Hz) measurements as a function of measuring temperature for the sample isothermally crystallized at 393 K. The dashed lines are guides for the eye

the α-relaxation with respect to the β-relaxation and conductivity is very important for the determination of relaxation strength. We have done this very precisely by extrapolating curve shape and peak position of the β-relaxation and conductivity from temperatures where we can observe these effects separately (low and high temperatures, respectively) to the temperature where we observe the α-relaxation [30].

In spite of all uncertainties we do not find any indication of a separate glass transition while increasing temperature neither from calorimetric nor from dynamic measurements. The question arises what is the reason for the glassy state of the rigid amorphous fraction? To answer the question, our image is the following: while cooling a polymer from the melt, crystallization occurs at T_c. At the same moment, the mobility of the chains in the immediate vicinity of the lamellae is drastically reduced. No co-operative movements are possible which means that the chains are vitrified. The material behaves as a glass as shown in Fig. 8 [3]. The remaining liquid mobile amorphous material vitrifies at lower temperatures comparable with that of a bulky amorphous sample (T_g).

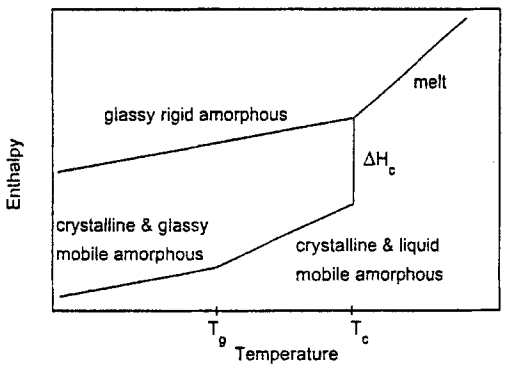

Fig. 8 Schematic plot of enthalpy as function of temperature for the different fractions of a semi-crystalline polymer

To illustrate vitrification by partial crystallization heating and cooling scans for the low molecular weight compound 2,5-bis(2-dodecyloxycarbonylphenylthio)terephthalic dodecyl diester are given in Fig. 9. From both heating as well as cooling scans a superposition of glass transition and melting or crystallization, respectively can be seen. The heat of fusion of about 12 kJ mol^{-1} shows that only a small part of the molecule, may be parts of the alkane chains, are involved in this crystallization. The observed melting temperature of 246 K corresponds to a crystallized alkane chain of about 10 carbon atoms [35, 36]. We will investigate this in more detail in the future. For the totally crystalline compound a heat of fusion of about 123 kJ mol^{-1} was obtained.

The glass transition as well as the fusion peak is shifted by 7 K between heating and cooling. Because the temperature axis is corrected to thermal lag effects (about 2 K) the origin of this difference can not be the glass transition. Neglecting differences in the curve shape, the glass transition normally occurs at the same tempera-

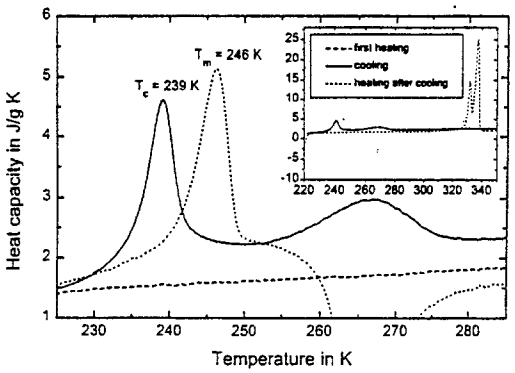

Fig. 9 Heating and cooling scans in the glass transition region of 2,5-bis(2-dodecyloxycarbonylphenylthio)terephthalic dodecyl diester. Heating rate ±10 K min^{-1}; sample mass 2.4 mg. The inset shows additional cold crystallization and melting

ture for cooling and heating. The observed difference can be related to the supercooling of crystallization of alkane chains. That means we observe the vitrification (devitrification) of the whole molecule (Δc_p=490 J $mol^{-1}K^{-1}$) due to the crystallization (melting) of a small part of it.

Temperature modulated measurements support this picture because we do not observe a frequency dependence of the glass transition in the real part of the complex heat capacity. This result shows that there is a vitrification as well as devitrification due to crystallization (immobilization) or melting (mobilization), respectively of a small part of the molecule. For this compound during partial crystallization, the whole non-crystalline fraction becomes rigid amorphous. It becomes glassy at higher temperatures than expected from the homologues and no vitrification (devitrification) due to temperature changes without change in the crystalline structure can be observed. From the homologues an extrapolated T_g of about 140 K is expected [13] but vitrification is observed at about 240 K. We think in principle the same happens for most of the semi-crystalline polymers. To clarify this further investigations are necessary.

From another point of view, this result is important too. If immobilization of a small part of the molecule results in vitrification of the whole molecule a co-operative motion is necessary for mobilization (glass transition). Because local movements are still present in partially crystalline systems, this supports the idea of the co-operative nature of glass transition.

Conclusion

Investigations of the glass transition in semi-crystalline PET other than calorimetric also yield a rigid amorphous fraction. Qualitatively the same results can be observed by different investigations of dynamic glass transition (relaxation). Comparison of mobile amorphous fraction from vitrification (Δc_{pDSC}) with that es-

timated from relaxation strength of dielectric- and dynamic mechanical spectroscopy as well as, temperature modulated calorimetry, shows no significant differences for two series of different crystallized PET. No temperature dependence of the mobile amorphous fraction could be seen from dielectric and dynamic mechanical measurements over a wide frequency range. We do not detect a separate glass transition for the rigid amorphous fraction until melting of crystals. The superposition of glass transition (vitrification, devitrification) with crystallization or melting is due to the immobilization of long range movements (modes) due to the fixation of molecule parts by the crystallites. Local movements as observed by the β-relaxation are only affected to a small extent by this fixation [30]. Observations on a low molecular weight model compound support the idea of crystallization (immobilization) induced glass transition in the vicinity of crystallites.

* * *

This work has been supported by the DFG and DAAD (A.M.G). The authors express their thanks to G.W.H. Höhne (Ulm) for fruitful discussions on crystallization of alkanes.

References

1 Y. Ishida, K. Yamafuji, H. Ito and M. Takayanagi, Koll.-Zeitsch. und Zeitsch. Polym., 184 (1962) 97.
2 H. Suzuki, J. Grebowicz and B. Wunderlich, Brit. Polym., J., 17 (1985) 1.
3 M. Alsleben and C. Schick, Thermochim. Acta, 238 (1994) 203.
4 E. Donth, Relaxation and Thermodynamics in Polymers, Glass Transition, Akademie Verlag, Berlin 1993.
5 J. Jäckle, J. Non-Cryst. Solids, 172 (1994) 104.
6 J. Dobbertin, A. Hensel and C. Schick, J. Thermal Anal., 47 (1996) 1027.
7 C. Schick, F. Fabry, U. Schnell, G. Stoll, L. Deutschbein and W. Mischok, Acta Polym., 39 (1988) 705.
8 E. W. Fischer and S. Fakirov, J. Mater. Sci., 11 (1976) 1041.
9 G. Groeninckx, H. Berghmans and G. Smets, J. Polym. Sci. Polym. Phys. Ed., 18 (1980) 1311.
10 G. Groeninckx and H. Berghmans, J. Polym. Sci. Polym. Phys. Ed., 18 (1980) 1325.
11 C. Schick and E. Donth, Physica Scripta, 43 (1991) 423.
12 C. Schick, L. Krämer und W. Mischock, Acta Polym., 36 (1985) 47.
13 M. Pötter, H. Dehne, H. Reinke, J. Dobbertin and C. Schick, Mol. Cryst. Liq. Cryst., submitted.
14 N. O. Birge and S. R. Nagel, Phys. Rev. Lett., 54 (1985) 2674.
15 N. O. Birge and S. R. Nagel, Rev. Sci. Instrum., 58 (1987) 1464.
16 R. Florian, J. Peilzl, M. Rosenberg, H. Vargas and R. Wernhardt, Phys. Status Solidi (a), 48 (1978) k35.
17 M. Nishikawa and Y. Saruyama, Thermochim. Acta, 267 (1995) 75.
18 M. Reading, Trends Polym. Sci., 8 (1993) 248.
19 J. E. K. Schawe, Thermochim. Acta, 261 (1995) 183.
20 A. Hensel and C. Schick, Thermochim. Acta, in preparation.
21 B. Wunderlich, Pure and Applied Chem., 67 (1995) 1919 see on the WWW (Internet), URL: http://funnelweb.utcc.utk.edu/~athas.
22 A. Hensel, J. Dobbertin, J. E. K. Schawe, A. Boller and C. Schick, J. Thermal Anal., 46 (1996) 935.
23 A. Boller, C. Schick and B. Wunderlich, Thermochim. Acta, 266 (1995) 97.

24 A. Boller, Y. Jin and B. Wunderlich, J. Thermal Anal., 42 (1994) 307.
25 F. Kremer, D. Boese, G. Meier and E. W. Fischer, Prog. Coll. Polym. Sci., 80 (1989) 129.
26 S. Havriliak and S. Negami, J. Polym. Sci. C, 14 (1966) 99.
27 E. Schlosser and A. Schönhals, Coll. Polym. Sci., 267 (1989) 963.
28 E. Schlosser, A. Schönhals, H. E. Carius and H. Goering, Macromolecules, 26 (1993) 6027.
29 J. C. Coburn and R. H. Boyd, Macromolecules, 19 (1986) 2238.
30 J. Dobbertin, Ph D, University of Rostock, 1995.
31 M. Arndt and F. Kremer, Mat. Res. Soc. Symp. Proc., 366 (1995) 259.
32 H. Schäfer, E. Sternin, R. Stannarius, M. Arndt and F. Kremer, Phys. Rev. Lett., 76 (1996) 2177.
33 E. Schlosser and A. Schönhals, Coll. Polym. Sci., 267 (1989) 963.
34 P. Cebe and P. P. Huo, Thermochim. Acta, 238 (1994) 229.
35 P. J. Flory, Trans. Faraday Soc., 51 (1955) 848.
36 W. Gerum, G. W. H. Höhne and W. Wilke, Macromol. Chem. Phys., 197 (1996) 1691.